JOURNAL OF SPACECRAFT AND ROCKETS
Vol. 37, No. 3, May–June 2000

Minimum-Variance Estimation of Reentry Debris Trajectories

Anil V. Rao*
The Aerospace Corporation, El Segundo, California 90245

A minimum-variance estimator is developed for reentry debris trajectories using discrete-time multiple sensor line-of-sight measurements. An integral state model is used for the unknown drag ballistic coefficient and lift ballistic coefficient. An extended Kalman filter is developed for the forward estimate and a Rauch–Tung–Striebel smoother is developed for the backward estimate. The method is tested on nonlifting and lifting reentry trajectories that are synthesized using a high-fidelity trajectory simulator. The results of this research show that reentry debris trajectories can be estimated using the approach developed despite the lack of accurate models for the aerodynamic coefficients.

Nomenclature

C_D = drag coefficient
C_L = lift coefficient
$\boldsymbol{D}$ = drag acceleration in Earth-centered inertial coordinate system (ECI), m/s^2
$E[\cdot]$ = expected value
F = linearized system matrix, $\partial \boldsymbol{f}/\partial \boldsymbol{x}$
$\boldsymbol{f}$ = right-hand side of dynamic model
$\boldsymbol{g}$ = gravitational acceleration in ECI, m/s^2
H = linearized measurement matrix, $\partial \boldsymbol{h}/\partial \boldsymbol{x}$
h = altitude over oblate Earth, m
$\boldsymbol{h}$ = right-hand side of measurement model
I_n = $n \times n$ identity matrix
J_2 = oblateness coefficient
K = Kalman filter gain
$\boldsymbol{L}$ = lift acceleration in ECI, m/s^2
$\boldsymbol{l}$ = line-of-sight vector in ECI, m
m = mass, kg
N = number of measurements
$\boldsymbol{n}$ = measurement process noise
P = error covariance
p = $\sqrt{\beta_D}$, m/kg$^{1/2}$
Q = spectral density
R_e = Earth equatorial radius, m
R_p = Earth polar radius, m
$\boldsymbol{r}$ = ECI position, m
S = reference area, m^2
T = transformation matrix
t = time, s
$\boldsymbol{v}$ = ECI velocity, m/s
$\boldsymbol{w}$ = dynamic model process noise
$\boldsymbol{x}$ = state
$\boldsymbol{x}_a$ = augmented state
$\hat{\boldsymbol{x}}$ = state estimate
$\hat{\boldsymbol{x}}_a$ = augmented state estimate
$\boldsymbol{z}$ = measurement, rad
α = altitude scale factor for air density, m^{-1}
β_D = drag ballistic coefficient, m^2/kg
β_L = lift ballistic coefficient, m^2/kg
θ = geocentric latitude, rad
μ = gravitational parameter, m^3/s^2
ρ = air density, kg/m^3
ρ_0 = air density at sea level, kg/m^3
σ = standard deviation
Φ = state transition matrix
ϕ = longitude, rad
χ = elevation in local horizontal coordinate system (LH), rad
ψ = azimuth in LH, rad
Ω = magnitude of Earth rotation rate, rad/s
$\boldsymbol{\omega}$ = Earth rotation rate vector, rad/s

Subscripts

er = quantity in Earth relative velocity coordinate system
er2e = Earth relative velocity coordinate system to ECI transformation
e2lh = ECI to LH transformation
k = sampling index
lh = quantity in local horizontal coordinate system
lh2e = LH to ECI transformation

Received 14 October 1999; revision received 11 February 2000; accepted for publication 2 March 2000.

*Senior Member of the Technical Staff, Flight Mechanics Department, 2350 E. El Segundo Boulevard; anilvrao@alumni.princeton.edu. Member AIAA.

Introduction

CURRENTLY, there are over 8500 nonoperational objects in space. This number grows every year due to the increasing frequency of new space missions. Many of these objects will interfere with future space missions, and others will survive reentry and pose a threat to terrestrial life.[1] Consequently, orbital and reentry debris are important problems in the space community.

Recently, the problem of orbital debris has received a great deal of attention.[2–4] By contrast, the reentry debris problem has received less attention. However, recent evidence shows that reentry debris also pose a great hazard. One such example is the second stage of a Delta rocket that reentered the Earth's atmosphere on 22 January 1997. Two large fragments from this rocket survived reentry: a stainless steel propellant tank that landed near a residence in Georgetown, Texas and a titanium helium tank that landed near Seguin, Texas.[5] Although no casualties resulted from this incident, the mere fact that these objects survived reentry demonstrates that debris are potentially hazardous to life on Earth. Mitigating such terrestrial hazards requires knowledge of the location of an object as it reenters the Earth's atmosphere. Consequently, it is important to develop methods to estimate reentry debris trajectories.

It is not possible to obtain an accurate estimate of a reentry trajectory without knowledge of the aerodynamic load. Therefore, it is necessary to specify an aerodynamic model for the object. Unfortunately, aerodyamic models are generally not known for reentry debris because the geometry and mass of the object are unknown. Consequently, it is not possible to use a prescribed aerodynamic model when estimating a trajectory for reentry debris. Instead, as part of the trajectory estimation, it is necessary to develop a procedure that simultaneously estimates the aerodynamic load. For reentry debris, the unknown parameters in the aerodynamic model are the reference area, coefficient of drag, coefficient of lift, and mass. These four parameters can be replaced by two quantities called the drag ballistic coefficient and the lift ballistic coefficient.[6] An estimate for the aerodynamic load can then be computed using the estimates of these ballistic coefficients.

Different approaches can be developed for estimating the ballistic coefficients. One possibility is to parameterize the ballistic coefficients using a particular functional form. Then the values of the parameters can be found that minimize a sum of squares of the measurement residuals. Such an approach is called nonlinear least-squares estimation.[7–9] The Trajectory Reconstruction Program[10] uses such an approach for estimating reentry trajectories.

Although a nonlinear least-squares approach may produce accurate results for some problems, often such results will be inaccurate due to an inappropriately chosen ballistic coefficient model. In principle, this limitation can be overcome by developing a large database of ballistic coefficient models, solving the least-squares problem using every model in the database, and subjectively choosing the best result. However, because the object properties are not known, it will be difficult to determine which result is closest to the actual reentry trajectory. Moreover, such an approach is cumbersome and may not be realizable in real time (which may be desirable in some situations).

An alternate approach to nonlinear least squares is minimum-variance estimation.[11,12] A minimum-variance estimator minimizes the estimation error using certain assumed statistical properties of the state, dynamics, and measurements. Minimum-variance estimation has several advantages over nonlinear least-squares estimation. One advantage is that relatively simple models can be developed for the unknown parameters, and these models can be applied to a relatively wide range of problems. Another advantage of minimum-variance estimation is that it can be used either in real time or offline.

Unlike nonlinear least-squares estimation, where unknown parameters are modeled deterministically, in minimum-variance estimation unknown parameters are modeled stochastically. A simple model that has been used successfully to estimate unknown parameters is the integral state model.[12–14] In an integral state model, the unknown parameters are modeled as integrals of a random disturbance input. The integral state is then adjoined to the original state, and the augmented state is estimated.

Minimum-variance estimation has been applied to several problems in atmospheric reentry. In Ref. 15 an extended Kalman filter is developed to track ballistic missiles trajectories using range, azimuth, and elevation measurements for a vehicle with a known aerodynamic model. In Ref. 16 a Kalman filter was developed to estimate ballistic missile reentries with uncertain drag. Common to these and other similar studies is that a great deal was known a priori about the aerodynamics. Moreover, the estimation methods developed in these studies relied on large amounts of measurement data that included both range and angular position information.

In this paper, a minimum-variance estimator is developed for reentry debris trajectories using azimuth and elevation measurements and with no a priori knowledge of the aerodynamic coefficients. The ballistic coefficients are modeled as integral state variables. The minimum-variance estimator is developed in the form of a two-pass smoother. An extended Kalman filter (EKF)[17] is developed for the forward estimate and a Rauch–Tung–Striebel (RTS) smoother[17] is developed for the backward estimate. The method can be used either in real time or offline. When a real-time estimate is desired, the EKF can be used alone. When an offline estimate is feasible, the backward smoother can be added to improve the forward estimate.

The performance of the estimator is assessed on both nonlifting and lifting reentry trajectories synthesized using the high-fidelity Generalized Trajectory Simulation[18] (GTS) program. The GTS trajectories are the exact solutions against which estimates are compared. Noisy line-of-sight measurements are synthesized along the exact solutions by use of a Gaussian random number generator. The estimator is then applied in exactly the same manner as would be required for an actual reentry.

Four cases are evaluated. First, an estimate of the nonlifting reentry trajectory is obtained with only the drag ballistic coefficient modeled as an integral state. Second, an estimate of the nonlifting reentry trajectory is obtained with both the drag ballistic coefficient and the lift ballistic coefficient modeled as integral states. Third, an estimate of the lifting reentry trajectory is obtained using the same approach as in the first case. Fourth, an estimate of the lifting reentry trajectory is obtained using the same approach as in the second case. The results of this research demonstrate that the approach developed here is a viable way to estimate reentry debris trajectories despite the lack of accurate models for the aerodynamic coefficients.

Minimum-Variance Estimation

A minimum-variance estimator in the form of a two-pass smoother is now developed. An EKF is developed for the forward estimate whereas an RTS smoother is developed for the backward estimate.

Forward Estimate: EKF

In this paper we consider the continuous-discrete form of the EKF (see Ref. 12 for more details). The EKF computes minimum-variance estimates for nonlinear dynamic systems of the form

$$\dot{\boldsymbol{x}} = \boldsymbol{f}[\boldsymbol{x}, t] + \boldsymbol{w} \tag{1}$$

where $\boldsymbol{f}$ is a nonlinear function of $\boldsymbol{x}$, and $\boldsymbol{w}$ is a zero-mean Gaussian white-noise random process, that is,

$$E[\boldsymbol{w}(t)] = 0, \qquad E[\boldsymbol{w}(t)\boldsymbol{w}^T(\tau)] = Q(t)\delta(t-\tau) \tag{2}$$

where $\delta(\cdot)$ is the Dirac delta function and $Q(t)$ is the spectral density or finite intensity of $\boldsymbol{w}$. Discrete-time measurements of the form

$$z_k = \boldsymbol{h}[\boldsymbol{x}(t_k)] + \boldsymbol{n}_k, \qquad k = 1, 2, \ldots, N \tag{3}$$

are taken at times $t \in [t_1, \ldots, t_N]$, where $\boldsymbol{n}_k$ is a zero-mean Gaussian white-noise random process, that is,

$$E[\boldsymbol{n}_k] = 0, \qquad E\left[\boldsymbol{n}_k \boldsymbol{n}_l^T\right] = \begin{cases} R_k, & l = k \\ 0, & l \neq k \end{cases} \tag{4}$$

The state estimate and its error covariance are defined, respectively, as

$$\hat{\boldsymbol{x}} = E[\boldsymbol{x}] \tag{5}$$

$$P = E[(\boldsymbol{x} - \hat{\boldsymbol{x}})(\boldsymbol{x} - \hat{\boldsymbol{x}})^T] \tag{6}$$

Furthermore, it is assumed that the initial state estimate and the initial error covariance, $\hat{\boldsymbol{x}}_0$ and P_0, respectively, are known. The EKF propagates the state estimate and its error covariance from t_{k-1} to t_k by integrating the system of differential equations

$$\dot{\hat{\boldsymbol{x}}} = \boldsymbol{f}[\hat{\boldsymbol{x}}, t], \qquad \dot{P} = FP + PF^T + Q \tag{7}$$

with the initial conditions

$$\hat{\boldsymbol{x}}(t_{k-1}) = \hat{\boldsymbol{x}}_{k-1}^+, \qquad P(t_{k-1}) = P_{k-1}^+ \tag{8}$$

where

$$F[\hat{\boldsymbol{x}}(t)] = \left(\frac{\partial \boldsymbol{f}}{\partial \boldsymbol{x}}\right)_{x(t)=\hat{x}(t)}, \qquad H[\hat{\boldsymbol{x}}(t)] = \left(\frac{\partial \boldsymbol{h}}{\partial \boldsymbol{x}}\right)_{x(t)=\hat{x}(t)} \tag{9}$$

and $\hat{\boldsymbol{x}}(t)$ is the estimate at time t. At $t = t_k$, the state estimate and error covariance are updated, respectively, as

$$\hat{\boldsymbol{x}}_k^+ = \hat{\boldsymbol{x}}_k^- + K_k\left\{z_k - \boldsymbol{h}\left[\hat{\boldsymbol{x}}_k^-\right]\right\} \tag{10}$$

$$P_k^+ = \left\{I_n - K_k H_k^-\right\} P_k^- \tag{11}$$

where

$$K_k = P_k^-\left[H_k^-\right]^T\left\{H_k^- P_k^-\left[H_k^-\right]^T + R_k\right\}^{-1} \tag{12}$$

is the Kalman filter gain and the notation $(\cdot)_k^-$ and $(\cdot)_k^+$ denote quantities before and after the kth measurement, respectively.

Backward Estimate: RTS

Assume that a forward filter estimate from an EKF is available. The forward filter state estimate $\hat{\boldsymbol{x}}_k$, $k = 1, \ldots, N$, and error covariance P_k, $k = 1, \ldots, N$, are given as

$$\hat{\boldsymbol{x}}_k = \hat{\boldsymbol{x}}_k^+, \qquad P_k = P_k^+, \qquad k = 1, \ldots, N$$

Let the smoothed state estimate and error covariance be denoted $\hat{\boldsymbol{x}}_{k|N}$ and $P_{k|N}$, respectively. The boundary conditions for the smoothed state estimate and error covariance are the EKF outputs at $t = t_N$, that is,

$$\hat{\boldsymbol{x}}_{N|N} = \hat{\boldsymbol{x}}_N^+, \qquad P_{N|N} = P_N^+ \tag{13}$$

Although there are several forms for fixed-interval backward smoothing, in this paper we consider the RTS smoother because it is more convenient to mechanize than other fixed-interval smoothing methods in that it does not require inverting an error covariance matrix.[12] In terms of the forward filter estimate and the smoothed estimate at stage $k + 1$, the smoothed estimate at stage k is given as[12]

$$\hat{\boldsymbol{x}}_{k|N} = \hat{\boldsymbol{x}}_k + K_{k|N}\{\hat{\boldsymbol{x}}_{k+1|N} - \Phi_k \hat{\boldsymbol{x}}_k - \boldsymbol{b}_k\}$$

$$K_{k|N} = P_k \Phi^T \left\{\Phi P_k \Phi_k^T + Q_k\right\}^{-1}, \qquad k = N - 1, \ldots, 1$$

$$P_{k|N} = P_k + K_{k|N}\left\{P_{k+1|N} - \Phi_k P_k \Phi_k^T\right\} K_{k|N}^T \tag{14}$$

where $\boldsymbol{b}_k$ is the solution of the differential equation

$$\dot{\boldsymbol{b}} = F[\hat{\boldsymbol{x}}(t)]\boldsymbol{b} + \boldsymbol{f}[\hat{\boldsymbol{x}}(t), t] - F[\hat{\boldsymbol{x}}(t)]\hat{\boldsymbol{x}}(t), \qquad \boldsymbol{b}(t_k) = 0 \tag{15}$$

at time t_{k+1}, Φ_k is the state transition matrix of $F[\hat{\boldsymbol{x}}(t)]$ from t_k to t_{k+1}, and

$$Q_k = \int_{t_k}^{t_{k+1}} \Phi(s, t_k) Q(s) \Phi^T(s, t_k)\, \mathrm{d}s \tag{16}$$

Estimator Dynamic and Measurement Models

Models are now developed for use in the minimum-variance estimator described in the preceding section. In the first subsection the estimator dynamic model is developed, and in the second subsection the estimator measurement model is developed.

Estimator Dynamic Model

Consider an object reentering the Earth's atmosphere under the influence of gravity, drag, and lift. The three-degree-of-freedom equations describing the motion of the object are given in Earth-centered inertial (ECI) coordinates as

$$\dot{\boldsymbol{r}} = \boldsymbol{v}, \qquad \dot{\boldsymbol{v}} = \boldsymbol{g} + \boldsymbol{D} + \boldsymbol{L} \tag{17}$$

where $\boldsymbol{r} = [x \;\; y \;\; z]^T$ and $\boldsymbol{v} = [\dot{x} \;\; \dot{y} \;\; \dot{z}]^T$. For the duration over which the reentry trajectory will be estimated, it is sufficiently accurate to model the gravitational acceleration using the central body and oblateness effects. Consequently, $\boldsymbol{g}$ is given as[19]

$$\boldsymbol{g} = \begin{bmatrix} -\mu(x/r^3)\left\{1 + \frac{3}{2}J_2(R_e/r)^2[1 - 5(z/r)^2]\right\} \\ -\mu(y/r^3)\left\{1 + \frac{3}{2}J_2(R_e/r)^2[1 - 5(z/r)^2]\right\} \\ -\mu(z/r^3)\left\{1 + \frac{3}{2}J_2(R_e/r)^2[3 - 5(z/r)^2]\right\} \end{bmatrix} \tag{18}$$

where $r = \|\boldsymbol{r}\|_2$ and $\|\cdot\|_2$ is the Euclidean norm. When we assume that all lift acts vertically in the Earth relative velocity (ER) coordinate system (see Fig. 1), the drag and lift accelerations in ER are given, respectively, as

$$\boldsymbol{D}_{\mathrm{er}} = \begin{bmatrix} -D \\ 0 \\ 0 \end{bmatrix} \tag{19}$$

Table 1 Constants for use in estimator dynamic model

Quantity	Numerical value
R_e, m	6,378,145.0
R_p, m	6,356,752.0
α, m^{-1}	1.39951×10^{-4}
μ, $\mathrm{m}^3/\mathrm{s}^2$	3.986×10^{14}
Ω, rad/s	7.2921×10^{-5}
ρ_0, kg/m^3	1.2263

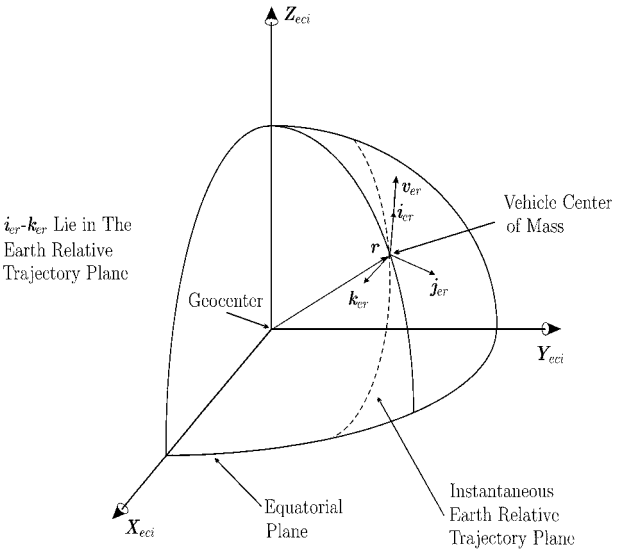

Fig. 1 Geometry of the ER coordinate system.

$$\boldsymbol{L}_{\mathrm{er}} = \begin{bmatrix} 0 \\ 0 \\ -L \end{bmatrix} \tag{20}$$

where

$$D = \tfrac{1}{2}\rho v_{\mathrm{er}}^2 S C_D / m, \qquad L = \tfrac{1}{2}\rho v_{\mathrm{er}}^2 S C_L / m \tag{21}$$

where $\boldsymbol{v}_{\mathrm{er}} = \boldsymbol{v} - \boldsymbol{\omega} \times \boldsymbol{r}$ is the ER velocity, $\boldsymbol{\omega} = [0 \;\; 0 \;\; \Omega]^T$, and $v_{\mathrm{er}} = \|\boldsymbol{v}_{\mathrm{er}}\|_2$. When we use the transformation T_{er2e} (see Appendix), the lift and drag accelerations in the ECI coordinate system are given as

$$\boldsymbol{D} = T_{\mathrm{er2e}}\boldsymbol{D}_{\mathrm{er}}, \qquad \boldsymbol{L} = T_{\mathrm{er2e}}\boldsymbol{L}_{\mathrm{er}} \tag{22}$$

The density is assumed to be exponential of the form

$$\rho = \rho_0 \exp(-\alpha h) \tag{23}$$

where h is the altitude over an oblate Earth modeled as

$$h = r - R_e \Big/ \sqrt{1 + (z^2/r^2)\left(R_e^2 / R_p^2 - 1\right)} \tag{24}$$

The values of various constants that are used in the estimator dynamic model are given in Table 1.

For reentry debris, the parameters S, C_D, C_L, and m are all unknown. These four parameters can be reduced to two parameters β_D and β_L given as

$$\beta_D = SC_D/m, \qquad \beta_L = SC_L/m \tag{25}$$

The quantities β_D and β_L are the drag ballistic coefficient and lift ballistic coefficient, respectively.[6] Because $\boldsymbol{L}$ can be directed either upward or downward, β_L can be either positive or negative. However, because $\boldsymbol{D}$ always acts opposite $\boldsymbol{v}_{\mathrm{er}}$, β_D must be nonnegative. Consequently, the substitution $p^2 = \beta_D$ is made. The values of D and L are then given as

$$D = \tfrac{1}{2}\rho v_{\mathrm{er}}^2 p^2, \qquad L = \tfrac{1}{2}\rho v_{\mathrm{er}}^2 \beta_L \tag{26}$$

Because p and β_L are unknown, they must be estimated along with $\boldsymbol{r}$ and $\boldsymbol{v}$. A simple model that has been used successfully to estimate unknown parameters is the integral state model.[12–14] In an integral state model, any unknown parameter is modeled as a cascade of integrals of a zero-mean Gaussian white-noise process. For the best estimator performance, the minimum number of integrals should be chosen. Because p and β_L are required in this application, a single integral is sufficient. Consequently, the dynamics of p and β_L are given by

$$\begin{pmatrix} \dot{p} \\ \dot{\beta}_L \end{pmatrix} = \begin{pmatrix} w_D \\ w_L \end{pmatrix} = \boldsymbol{w}_\beta \tag{27}$$

where the integral state associated with p and β_L, denoted $\boldsymbol{x}_\beta$, is

$$\boldsymbol{x}_\beta = \begin{pmatrix} p \\ \beta_L \end{pmatrix} \tag{28}$$

$$E[\boldsymbol{w}_\beta] = 0, \qquad E\left[\boldsymbol{w}_\beta(t)\boldsymbol{w}_\beta^T(\tau)\right] = Q_\beta(t)\delta(t-\tau) \tag{29}$$

We assume here that w_D and w_L are uncorrelated and that Q_β is constant. Consequently,

$$Q_\beta(t) = Q_\beta = \begin{pmatrix} q_D & 0 \\ 0 & q_L \end{pmatrix} \tag{30}$$

The dynamics of $\boldsymbol{x}_\beta$ can then be written as

$$\dot{\boldsymbol{x}}_\beta = \boldsymbol{w}_\beta \tag{31}$$

The dynamics of the augmented state $\boldsymbol{x}_a$ then have the form

$$\dot{\boldsymbol{x}}_a = \boldsymbol{f}_a[\boldsymbol{x}_a, t] + \boldsymbol{w}_a \tag{32}$$

where

$$\boldsymbol{x} = \begin{pmatrix} \boldsymbol{r} \\ \boldsymbol{v} \end{pmatrix}, \qquad \boldsymbol{x}_a = \begin{pmatrix} \boldsymbol{x} \\ \boldsymbol{x}_\beta \end{pmatrix}, \qquad \boldsymbol{f}_a[\boldsymbol{x}_a, t] = \begin{pmatrix} \boldsymbol{f}[\boldsymbol{x}_a] \\ 0 \end{pmatrix}$$

$$\boldsymbol{w}_a = \begin{pmatrix} 0 \\ \boldsymbol{w}_\beta \end{pmatrix} \tag{33}$$

It is seen that Eq. (32) has the same form as Eq. (1). Because p and β_L are unknown, the intensities q_D and q_L of the white-noise processes become design parameters. Because each reentry has unique aerodynamic characteristics, q_D and q_L will be different for every problem. To this point, no systematic way has been found to choose q_D and q_L; they are chosen through trial and error.

Estimator Measurement Model

Measurements are acquired in the form of azimuth and elevation angles, denoted ψ and χ, respectively, in the local horizontal (LH) coordinate system of each sensor (Fig. 2). The angles χ and ψ are defined as follows. At the time of a measurement, the line-of-sight vector from the sensor to the object in the ECI coordinate system is

$$\boldsymbol{l} = \boldsymbol{r} - \boldsymbol{r}_s \tag{34}$$

where $\boldsymbol{r}_s$ is the ECI position of the sensor. The vector $\boldsymbol{l}$ is transformed from ECI to LH via the transformation T_{e2lh} (see Appendix) as

$$\boldsymbol{l}_{\text{lh}} = T_{\text{e2lh}}\boldsymbol{l} \tag{35}$$

Finally, the vector $\boldsymbol{l}_{\text{lh}}$ can be expressed in terms of the angles ψ and χ as

$$\boldsymbol{l}_{\text{lh}} = l_{\text{lh}} \begin{bmatrix} \sin\chi\cos\psi \\ \sin\chi\sin\psi \\ \cos\chi \end{bmatrix} \tag{36}$$

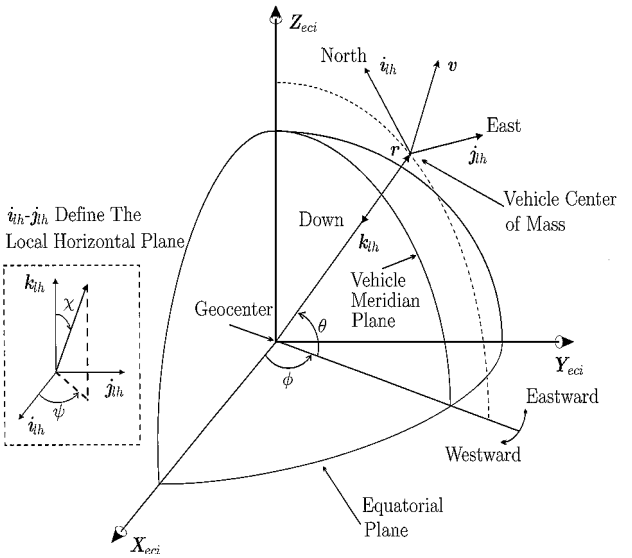

Fig. 2 Geometry of the LH coordinate system.

where ψ is the angle measured eastward from $\boldsymbol{i}_{\text{lh}}$ in the $\boldsymbol{i}_{\text{lh}}$–$\boldsymbol{j}_{\text{lh}}$ plane and χ is the angle between $\boldsymbol{l}_{\text{lh}}$ and $\boldsymbol{k}_{\text{lh}}$ (Fig. 2). The resulting measurement model is

$$\boldsymbol{h}[\boldsymbol{x}_a] = \begin{pmatrix} \psi \\ \chi \end{pmatrix} \tag{37}$$

where $\boldsymbol{x}_a$ is the augmented state as described in the preceding section. Finally, ψ and χ are modulated to lie between $[-\pi, \pi]$ and $[0, \pi]$, respectively.

Let the number of sensors for a given reentry be denoted m, where sensor i, $i = 1, \ldots, m$, takes n_i readings at times $t_{i,j}$, $j = 1, \ldots, n_i$ (which, in general, implies that the sensors are not synchronized). It is assumed that measurement errors in ψ and χ are each zero-mean Gaussian white-noise random processes with variances σ_ψ^2 and σ_χ^2, respectively, and that errors in ψ and χ are uncorrelated. At $t = t_k$ the measurement vector $\boldsymbol{z}_k$ has the form

$$\boldsymbol{z}_k = \boldsymbol{h}(\boldsymbol{x}_{a,k}) + \boldsymbol{n}_k \tag{38}$$

where $\boldsymbol{n}_k$ has the properties

$$E[\boldsymbol{n}_k] = 0, \qquad E\left[\boldsymbol{n}_k\boldsymbol{n}_l^T\right] = \begin{cases} R, & l = k \\ 0, & l \neq k \end{cases} \tag{39}$$

Furthermore, the error covariance matrix R has the form

$$R = \begin{pmatrix} \sigma_\psi^2 & 0 \\ 0 & \sigma_\chi^2 \end{pmatrix} \tag{40}$$

and is assumed to be constant. Note that Eq. (38) has the same form as Eq. (3).

Application of Estimator to a Synthesized Reentry

The minimum-variance estimator is now applied to two reentries that are synthesized using the GTS program.[18] The trajectories computed using GTS are considered the exact solutions (or exact trajectories) against which the estimated trajectories are compared.

Computation of Exact Solutions

Two exact solutions are computed using GTS: one corresponding to a nonlifting reentry (where the object experiences drag but not lift) and a lifting reentry (where the object experiences both drag and lift). The exact nonlifting reentry trajectory is computed by use of the following piecewise constant drag ballistic coefficient:

$$\beta_D = \begin{cases} 0.000318\ \text{m}^2/\text{kg}, & h > 74\ \text{km} \\ 0.000127\ \text{m}^2/\text{kg}, & h \leq 74\ \text{km} \end{cases} \tag{41}$$

The exact lifting reentry trajectory is computed by use of the same drag ballistic coefficient as in Eq. (41), but a lift-to-drag ratio of 0.1 is added, that is, β_L for the exact lifting reentry trajectory is given as

$$\beta_L = \beta_D / 10 \tag{42}$$

Furthermore, the exact solutions are all computed using the initial condition:

$$\boldsymbol{r} = \begin{bmatrix} -3{,}248{,}920.9291 \text{ m} \\ -5{,}651{,}764.6070 \text{ m} \\ 365{,}788.453 \text{ m} \end{bmatrix}, \qquad \boldsymbol{v} = \begin{bmatrix} 6836.047 \text{ m/s} \\ -3821.944 \text{ m/s} \\ -530.927 \text{ m/s} \end{bmatrix} \tag{43}$$

Finally, a 1962 U.S. standard atmosphere model is used in the computation of all exact solutions.

A piecewise constant drag ballistic coefficient is used to compute the exact solutions because it simulates an object breaking up in the Earth's atmosphere. In Eq. (41), the drag ballistic coefficient for altitudes above 74 km (approximate 40 nmile) represents an object that is intact, whereas the drag ballistic coefficient for altitudes below 74 km represents one of its pieces following breakup. It is known from experience that many objects break up at an altitude of approximately 74 km.

Computation of Noisy Measurements

Two sets of asynchronous measurements of ψ and χ are synthesized along the exact nonlifting and lifting reentry trajectories. The first set of measurements, labeled measurement set 1, is synthesized along the exact nonlifting reentry trajectory whereas the second set of measurements, labeled measurement set 2, is synthesized along the exact lifting reentry trajectory. Each set of measurements is synthesized by the use of four satellite sensors that employ the measurement model described in the preceding section. Measurements are corrupted with noise from a Gaussian random number generator using an error covariance:

$$R = \begin{pmatrix} 10^{-8} & 0 \\ 0 & 9 \times 10^{-8} \end{pmatrix} \text{rad}^2 \tag{44}$$

Finally, sensors 1, 2, 3, and 4 begin taking measurements at times, $t = 700$, 705.145, 708.89, and 703.648 s, respectively, at sampling frequencies of 0.087, 0.0725, 0.0658, and 0.1099 Hz, respectively. The sampling frequencies used in this example are similar to those found on real sensors. The sensor geometry for this problem is shown in Fig. 3.

The minimum-variance estimator is applied to both the nonlifting and lifting reentry trajectories. In all applications of the estimator, the dynamic and measurement models developed in the preceding section are used. In particular, the models for the ballistic coefficients are not those that are used to compute the exact solutions, but are estimated by use of the integral state model developed in the preceding section. The nonlifting reentry trajectory is estimated by the use of measurement set 1, whereas the lifting reentry trajectory is estimated by the use of measurement set 2. When applied in this manner, the estimator has no knowledge of the correct values of the ballistic coefficients.

The estimator is applied to the following four cases: 1) when measurement set 1 is used and the nonlifting reentry trajectory is estimated by including p in the integral state model, but excluding β_L from the integral state model; 2) when measurement set 1 is used and the nonlifting reentry trajectory is estimated by including both p and β_L in the integral state model; 3) when measurement set 2 is used and the lifting reentry trajectory is estimated by including p in the integral state model, but excluding β_L from the integral state model; and 4) when measurement set 2 is used and the lifting reentry trajectory is estimated by including both p and β_L in the integral state model. For all four cases, the initial error covariance is

$$P_0 = \text{diag}(930 \text{ m}^2, 930 \text{ m}^2, 930 \text{ m}^2, 9.3 \text{ m}^2/\text{s}^2, 9.3 \text{ m}^2/\text{s}^2, 9.3 \text{ m}^2/\text{s}^2, 0, 0) \tag{45}$$

where the last two entries of the diagonal in Eq. (45) are the initial error variances for p and β_L, respectively.

Case 1: Nonlifting Reentry Trajectory with p Estimated and $\beta_L \equiv 0$

The estimator is first demonstrated on a nonlifting reentry where only p is estimated, that is, β_L is set to zero. The quantities q_D and q_L are chosen as

$$q_D = 1.75 \times 10^{-4} \text{ m}^2/(\text{kg} \cdot \text{s}), \qquad q_L = 0 \tag{46}$$

The estimates of altitude and velocity are shown alongside the corresponding exact solutions in Figs. 4 and 5, respectively. Note that the estimates and their respective exact solutions are in close agreement. The smoothed estimation error in p is shown in Fig. 6 alongside the $\pm 3\sigma$ (99% confidence interval) error bound of the smoothed error covariance. The $\pm 3\sigma$ error bound is chosen because the smoothed

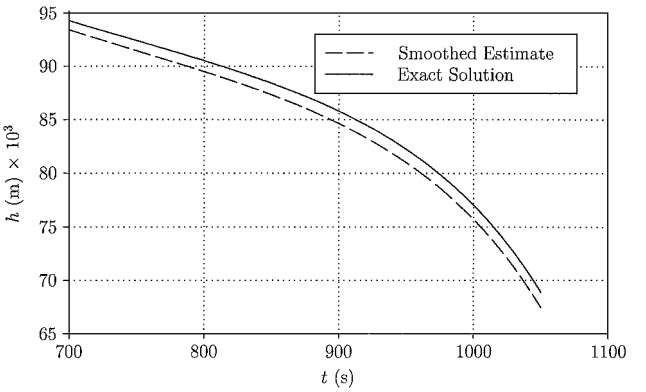

Fig. 4 Smoothed estimate of altitude alongside exact solution for case 1: nonlifting reentry with only p estimated.

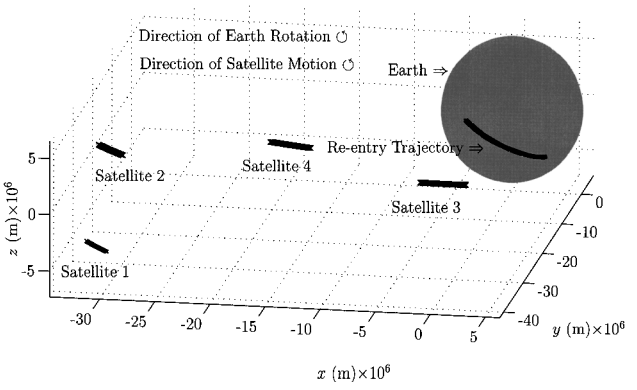

Fig. 3 Sensor geometry for simulated reentry in the ECI coordinate system.

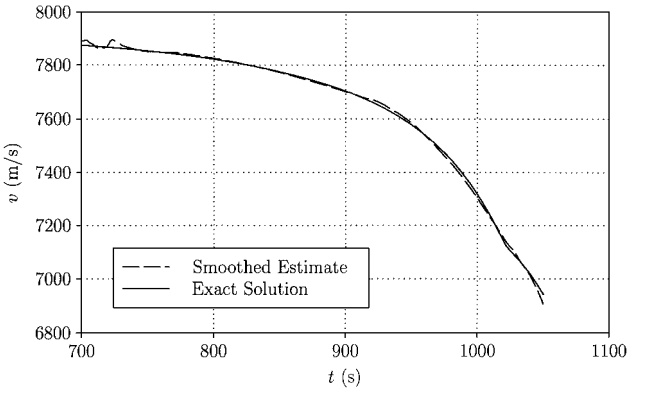

Fig. 5 Smoothed estimate of velocity alongside exact solution for case 1: nonlifting reentry with only p estimated.

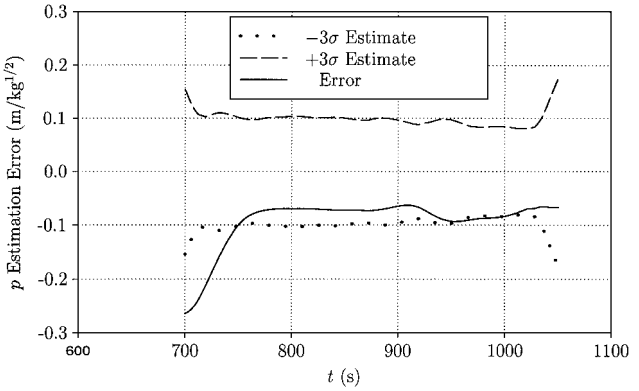

Fig. 6 Estimation error in p alongside ± 3σ estimate for case 1: nonlifting reentry with only p estimated.

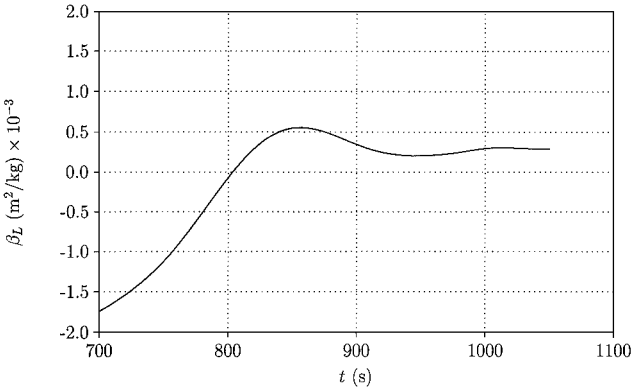

Fig. 8 Estimate of β_L for case 2: nonlifting reentry with both p and β_L estimated.

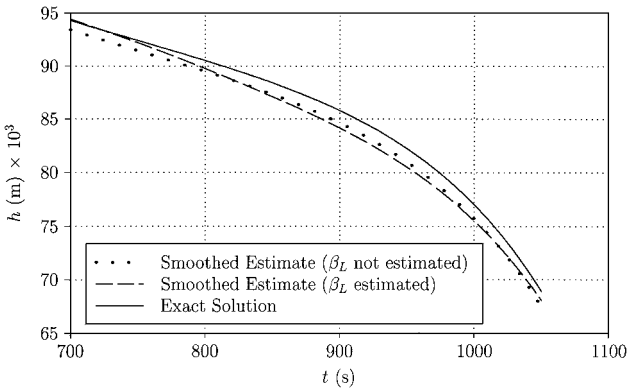

Fig. 7 Smoothed estimate of altitude alongside exact solution for case 1: nonlifting reentry with p as only parameter estimated and case 2: nonlifting reentry with both p and β_L estimated.

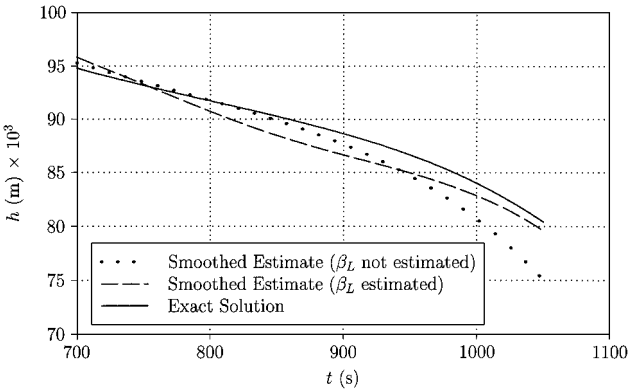

Fig. 9 Smoothed estimate of altitude alongside exact solution for case 3: lifting reentry with p as only parameter estimated and case 4: lifting reentry with both p and β_L estimated.

error covariance is only approximate[12] and, hence, it is better to use a more conservative bound for performance prediction. Moreover, it can be seen that the $\pm 3\sigma$ error bound is a good predictor of performance.

Case 2: Nonlifting Reentry Trajectory with Both p and β_L Estimated

Because it is not known a priori whether a reentry trajectory is lifting or nonlifting, it is generally necessary to estimate both p and β_L. For the particular case of a nonlifting reentry, it should be possible to obtain an accurate estimate of the reentry trajectory regardless of whether β_L is included or excluded. Consider again the same nonlifting reentry trajectory as in case 1. This time, however, consider an application of the estimator where both p and β_L are estimated. The quantities q_D and q_L are chosen as

$$q_D = 1.75 \times 10^{-4}\ \text{m}^2/(\text{kg}\cdot\text{s}), \qquad q_L = 1.11 \times 10^{-6}\ \text{m}^4/(\text{kg}^2\cdot\text{s}) \tag{47}$$

Figure 7 shows the estimated altitudes with β_L included and β_L excluded alongside the exact solution. Figure 8 shows the estimate of β_L itself. Note from Fig. 7 that the two altitude estimates are in close agreement and match very closely with the exact solution. Moreover, from Fig. 8, note that the estimate of β_L is small (on the order of 10^{-3} m^2/kg), which is consistent with the reentry trajectory being nonlifting.

Case 3: Lifting Reentry Trajectory with p Estimated and $\beta_L \equiv 0$

To demonstrate the need to estimate both p and β_L, consider a lifting reentry where only p is estimated, that is, β_L is set to zero. For this case, q_D and q_L are chosen as

$$q_D = 1.75 \times 10^{-4}\ \text{m}^2/(\text{kg}\cdot\text{s}), \qquad q_L = 0 \tag{48}$$

The estimated altitude of the lifting reentry with β_L excluded is shown in Fig. 9 (dotted line) alongside the exact solution (solid line). Unlike case 1, this time there is a large discrepancy between the estimated and exact altitudes. In particular, the estimated altitude is significantly lower than the exact altitude. The low estimate arises because the lift acceleration in the estimator dynamics is zero.

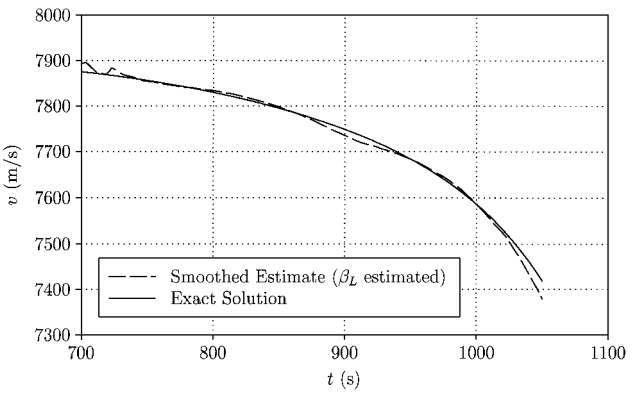

Fig. 10 Smoothed estimate of velocity alongside exact solution for case 4: lifting reentry with both p and β_L estimated.

Case 4: Lifting Reentry Trajectory with Both p and β_L Estimated

The poor performance of case 3 can be improved by estimating β_L. For this case q_D and q_L are chosen as

$$q_D = 1.75 \times 10^{-4}\ \text{m}^2/(\text{kg}\cdot\text{s}), \qquad q_L = 2.03 \times 10^{-7}\ \text{m}^4/(\text{kg}^2\cdot\text{s}) \tag{49}$$

Figures 9 and 10 show the altitude and velocity estimates for the lifting reentry trajectory when both p and β_L are estimated (dashed lines). A dramatic improvement in the estimate is seen over case 3. Whereas in case 3 the estimated and exact altitudes differed by over 6 km at the end of the trajectory, for this case the error is reduced to approximately 1 km. Furthermore, it is seen from Figs. 11 and 12

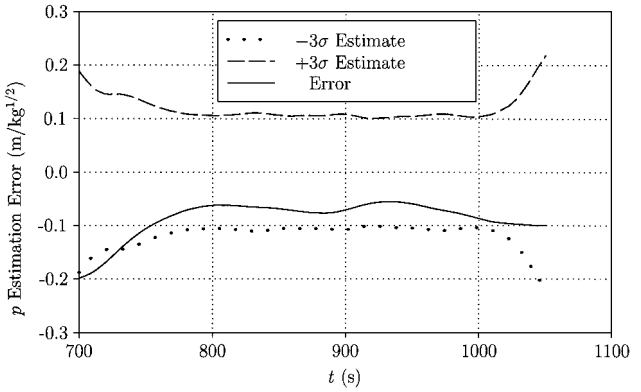

Fig. 11 Estimation error in p alongside ± 3σ estimate for case 4: lifting reentry with both p and β_L estimated.

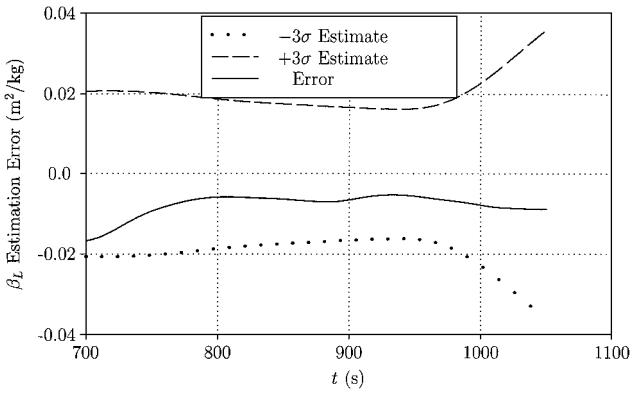

Fig. 12 Estimation error in β_L alongside ± 3σ estimate for case 4: lifting reentry with both p and β_L estimated.

that, similar to case 1, the estimates of p and β_L lie within their respective $\pm 3\sigma$ error bounds.

Discussion

Several important issues arise from the results. For nonlifting reentry trajectories, good estimator performance can be obtained either by estimating only p or by estimating both p and β_L. However, for lifting reentry trajectories, good estimator performance is obtained only when estimating both p and β_L. Therefore, it is preferable to use the more general estimator (i.e., one where both p and β_L are estimated) because the type of reentry trajectory is not known a priori. Moreover, note that an accurate estimate of the reentry trajectory can be obtained despite not having accurate models for the ballistic coefficients.

A feature of the approach used here is that it is extendible to other loads that may act on the object during reentry. Two examples of other loads are lateral lift and winds. Just as with the ballistic coefficients, these other two loads can be estimated by their being treated as integral states. Whereas these loads are usually small during a reentry, for some problems they may improve the accuracy of the estimated trajectory.

One of the purported advantages to using minimum-variance estimation is that the object may be tracked in real time. Real-time estimation can be accomplished by eliminating the backward smoother. Although the smoothed estimate will be more accurate than the forward estimate (everywhere except at the time of the final measurement where the two estimates are equal) when the estimator is applied in real time, only the most recent estimate is important. Consequently, in real time the improved accuracy obtained by the use of the backward smoother is of no added benefit.

Future Research and Analysis

Several topics for future research and analysis arise from the work presented here. Although a detailed study of each of these issues is beyond the scope of this paper, a brief discussion is warranted for completeness.

The location and sampling rate of sensors plays a key role in estimator performance. For certain reentries, the sensors may have poor line of sight, thereby they produce inaccurate estimates. Studying reentries with different sensor geometries will give insight into this issue. In addition, sensor sampling rate may effect estimator performance. There may be a threshold sampling rate below which the estimator may become unstable. Consequently, it is important to study the effect of sampling rate on estimator performance.

The ultimate goal of the method developed here is to estimate trajectories of actual reentries for which real sensor data is available. Currently, line-of-sight data from several such reentries is being acquired. By the use of these data, trajectory estimates will be computed and will be compared with other available information to assess their accuracy. The results of these analyses will help to gain confidence in the method.

One potential use of the results obtained here is to determine the probability distribution of the impact location of those objects that survive reentry. This determination may be made by the running of a Monte Carlo simulation, with the use of the final state estimate and error covariance as initial points from which to propagate the object to the surface of the Earth. Although this issue is beyond the scope of this paper, the results obtained here give a starting point for such an analysis.

Conclusions

A minimum-variance estimator has been developed for reentry debris trajectories. An integral-state model has been used for the unknown ballistic coefficients. An EKF has been developed for the forward estimate and an RTS smoother has been developed for the backward estimate.

The estimator has been applied to nonlifting and lifting reentry trajectories that were synthesized by the use of a high-fidelity trajectory simulator. It was found that an accurate estimate of the nonlifting reentry trajectory could be obtained either by estimating only the drag ballistic coefficient or by estimating both the drag ballistic coefficient and lift ballistic coefficient. However, for the lifting reentry it was necessary to estimate both the drag ballistic coefficient and lift ballistic coefficient to obtain an accurate estimate of the lifting reentry trajectory. The results of this research indicate that the approach developed here can be used to estimate reentry debris trajectories despite the lack of accurate aerodynamic models.

Appendix: Coordinate Transformations

ER to ECI

The geometry of the ER coordinate system is shown in Fig. 1. The transformation from ER to ECI, denoted T_{er2e}, is given as

$$T_{\text{er2e}} = [\boldsymbol{i}_{\text{er}} \quad \boldsymbol{j}_{\text{er}} \quad \boldsymbol{k}_{\text{er}}] \tag{A1}$$

where

$$\boldsymbol{i}_{\text{er}} = \frac{\boldsymbol{v}_{\text{er}}}{v_{\text{er}}}, \qquad \boldsymbol{j}_{\text{er}} = \frac{\boldsymbol{i}_{\text{er}} \times \boldsymbol{r}}{\|\boldsymbol{i}_{\text{er}} \times \boldsymbol{r}\|_2}$$

$$\boldsymbol{k}_{\text{er}} = \boldsymbol{i}_{\text{er}} \times \boldsymbol{j}_{\text{er}}, \qquad v_{\text{er}} = \|\boldsymbol{v}_{\text{er}}\|_2 \tag{A2}$$

LH to ECI

The geometry of the LH coordinate system is shown in Fig. 2. The ECI position $\boldsymbol{r}$ is expressed in terms of θ and ϕ as

$$\boldsymbol{r} = r \begin{bmatrix} \cos\theta\cos\phi \\ \cos\theta\sin\phi \\ \sin\theta \end{bmatrix} \tag{A3}$$

The transformation from LH to ECI, denoted T_{lh2e}, is given as

$$T_{\text{lh2e}} = [\boldsymbol{i}_{\text{lh}} \quad \boldsymbol{j}_{\text{lh}} \quad \boldsymbol{k}_{\text{lh}}] \tag{A4}$$

where

$$\boldsymbol{k}_{\text{lh}} = -\frac{\boldsymbol{r}}{r}, \qquad \boldsymbol{i}_{\text{lh}} = \begin{bmatrix} -\cos\phi\sin\theta \\ -\sin\phi\sin\theta \\ \cos\theta \end{bmatrix}$$

$$\boldsymbol{j}_{\text{lh}} = \boldsymbol{k}_{\text{lh}} \times \boldsymbol{i}_{\text{lh}}, \qquad r = \|\boldsymbol{r}\|_2 \tag{A5}$$

Consequently, $T_{\text{e2lh}} = T_{\text{lh2e}}^{T}$ is the transformation from the ECI to LH where $(\cdot)^T$ denotes matrix transpose.

Acknowledgments

This work was supported by the Center for Orbital and Re-Entry Debris Studies (CORDS) at The Aerospace Corporation. The author acknowledges the CORDS director, William Ailor, for supporting this research. The author also acknowledges Thomas Powell, John Cox, Vladimir Chobotov, and Ryan Noguchi for their helpful comments and suggestions during the preparation of the manuscript. Finally, the author acknowledges Walter Lillo for his guidance on many of the critical implementation issues.

References

[1]*Orbital Debris: A Technical Assessment*, Committee on Space Debris, National Research Council, National Academy Press, Washington, DC, 1995, pp. 1–10.

[2]Alfriend, K. T., Akella, M. R., Frisbee, J., Foster, J. L., Lee, D.-K., and Wilkins, M., "Probability of Collision Error Analysis," *Space Debris*, Vol. 1, No. 1, 1999, pp. 21–35.

[3]Williamsen, J. E., Evans, H. J., and Schonberg, W. P., "Effect of Multi-Wall System Composition on Survivability for Spacecraft Impacted by Orbital Debris," *Space Debris*, Vol. 1, No. 1, 1999, pp. 37–43.

[4]Pardini, C., and Anselmo, L., "Assessing the Risk of Orbital Debris Impact," *Space Debris*, Vol. 1, No. 1, 1999, pp. 59–80.

[5]"Rocket Body Components Survive Reentry," *Orbital Debris Quarterly News*, Vol. 2, No. 2, NASA Johnson Space Center, 1997, p. 2.

[6]Battin, R. H., *An Introduction to the Mathematics and Methods of Astrodynamics*, AIAA, New York, 1987, p. 505.

[7]Jazwinski, A. H., *Stochastic Processes and Filtering Theory*, Academic, New York, 1970, pp. 150–158.

[8]Hartley, H. O., "The Modified Gauss–Newton Method for the Fitting of Nonlinear Regression Functions by Least Squares," *Technometrics*, Vol. 3, 1961, pp. 269–280.

[9]Hartley, H. O., "Exact Confidence Regions for the Parameters in Nonlinear Regression Laws," *Biometrika*, Vol. 51, 1964, pp. 347–353.

[10]Rademacher, M. J., *Trajectory Reconstruction Program User Manual*, The Aerospace Corp., TR-0076 (9320)-5, El Segundo, CA, Sept. 1975.

[11]Kalman, R. E., "A New Approach to Linear Filtering and Prediction Problems," *Journal of Basic Engineering*, Vol. 82D, March 1960, pp. 35–45.

[12]Gelb, A. (ed.), *Applied Optimal Estimation*, MIT Press, Cambridge, MA, 1974, pp. 182–189, 200–203, 281 and 282.

[13]Mulgund, S. S., and Stengel, R. F., "Optimal Nonlinear Estimation for Aircraft Flight Control in Wind Shear," *Automatica*, Vol. 32, No. 1, 1996, pp. 3–13.

[14]Bossi, J. A., and Bryson, A. E., "Disturbance Estimation for a STOL Transport During Landing," *Journal of Guidance, Control, and Dynamics*, Vol. 5, No. 3, 1982, pp. 258–262.

[15]Wagner, W. E., "Re-Entry Filtering, Prediction, and Smoothing," *Journal of Spacecraft and Rockets*, Vol. 3, No. 9, 1966, pp. 1321–1327.

[16]Cardillo, G. P., Mrstik, A. V., and Plambeck, T., "A Track Filter for Reentry Objects with Uncertain Drag," *IEEE Transactions on Aerospace and Electronic Systems*, Vol. 35, No. 2, 1999, pp. 394–409.

[17]Rauch, H. E., Tung, F., and Striebel, C. T., "Maximum Likelihood Estimates of Linear Dynamic Systems," *AIAA Journal*, Vol. 3, No. 8, 1965, pp. 1445–1450.

[18]"A Generalized Trajectory Simulation System," Vols. 1–5, The Aerospace Corp., TR-0075(5549)-1, El Segundo, CA, 30 June 1975.

[19]Bate, R. R., Mueller, D. D., and White, J. E., *Fundamentals of Astrodynamics*, Dover, New York, 1971, pp. 419–422.

C. A. Kluever
Associate Editor